Available online at www.sciencedirect.com
SCIENCE DIRECT
Journal of Molecular Structure 742 (2005) 123–130
Journal of MOLECULAR STRUCTURE
www.elsevier.com/locate/molstruc

Structure and barrier to internal rotation of 4-methylstyrene in the S_0- and S_1-state

Michael Schmitt[a,*], Christian Ratzer[a], Christoph Jacoby[b], W. Leo Meerts[c]

[a]*Heinrich-Heine-Universität, Institut für Physikalische Chemie, Universitätsstr 26.43.02, D-40225 Düsseldorf, Germany*
[b]*Heinrich-Heine-Universität, Institut für Herz- und Kreislaufphysiologie, D-40225 Düsseldorf, Germany*
[c]*Department of Molecular and Laser Physics, Institute for Molecules and Materials, Radboud University Nijmegen, P.O. Box 9010, NL-6500 GL, Nijmegen, The Netherlands*

Received 13 October 2004; revised 12 November 2004; accepted 4 January 2005
Available online 8 February 2005

Abstract

The rotationally resolved spectrum of the electronic origin of methylstyrene has been studied in order to obtain the geometric structure and the barriers to methyl torsion in the electronic ground and excited state. The spectrum has been analyzed using an automated assignment based on the Genetic Algorithm. The geometry is found to be quinoidally distorted upon electronic excitation, what is typical for *para*-disubstituted aromatic compounds. The V_3 and V_6 barriers and the torsional constant F for both electronic states have been determined from a combined fit of low resolution torsional bands and high resolution torsionally perturbed rovibronic spectrum.

PACS: 33.15.Hp; 33.20.Lg; 33.20.Wr; 82.20.Wt; 31.15.Ar

Keywords: High resolution UV spectroscopy; Structure determination; Excited state; Ab initio

1. Introduction

4-Methylstyrene (4-MS) represents an interesting molecular system with a two and threefold/sixfold torsional potential for the vinyl group and the methyl group, respectively [1,2]. The molecule belongs to the molecular symmetry group G_{12} and a mixed V_3/V_6 potential energy for the methyl torsion is expected. 4-Methylstyrene is an ideal model system to study the 'through ring' interaction of the methyl group and the vinyl group via the respective torsional potentials.

For styrene there is a long-standing discussion about the planarity of the molecule in the electronic ground state. While the conjugation interaction between the vinyl group and the aromatic ring tends to prefer a planar structure, the steric repulsion between the *ortho*-ring hydrogen and the β-vinylic hydrogen favors a nonplanar structure. Møller–Plesset perturbation calculations predict the vinyl group to be noncoplanar with the aromatic plane [3], while density functional theory with the B3LYP functional yields a planar equilibrium geometry [4]. Grassian et al. [5] found planarity of styrene and nonsterically hindered styrenes in both ground and electronically excited states using one-color time-of-flight mass spectroscopy in a molecular beam, while Cochran et al. [6] determined a nonplanar structure using gas-phase electron diffraction.

The rotational spectrum of styrene has been reported by Caminati et al. [7]. The small negative inertial defect of $-0.6958\ \mu\text{Å}^2$ quoted in this publication is consistent with a planar molecule exhibiting a low frequency large amplitude motion. Rotationally resolved fluorescence excitation spectra reported by Ribblett et al. [8] show planarity of styrene also for the electronically excited S_1-state.

For 4-methylstyrene the questions arises, if the large amplitude motion of the methyl group is coupled to

* Corresponding author. Tel.: +49 211 811 3681; fax: +49 211 811 5195.
E-mail addresses: mschmitt@uni-duesseldorf.de (M. Schmitt), leo.meerts@science.ru.nl (W. Leo Meerts).

0022-2860/$ - see front matter © 2005 Elsevier B.V. All rights reserved.
doi:10.1016/j.molstruc.2005.01.010

the torsional motion of the vinyl group. As both groups in *para* position are shielded sterically by the aromatic ring, the interaction between them must be of electronic nature.

We present the rotationally resolved spectrum of the electronic origin of 4-methylstyrene, which is split into an A- and an E-component due to the internal rotation of the methyl group. The experimental spectrum is analyzed using a genetic algorithm (GA) based automated fitting procedure, which is far superior to classical assignment techniques in case of very dense and complex spectra [9–11]. Ab initio calculations on the structures and the torsional potentials will be presented and compared to the spectroscopic results.

2. Experimental

The experimental set-up for the rotationally resolved laser-induced fluorescence (LIF) is described in detail elsewhere [12] Briefly, it consists of a ring dye laser (Coherent 899-21) operated with Rhodamine 110, pumped with 6 W of the 514 nm line of an Ar^+-ion laser. The light is coupled into an external folded ring cavity (Spectra Physics) for second harmonic generation (SHG). The molecular beam is formed by expanding 4-methylstyrene heated to 190 °C and seeded in 800 mbar of argon through a 100 μm hole into the vacuum. The molecular beam machine consists of three differentially pumped vacuum chambers that are linearly connected by skimmers (1 and 3 mm, respectively) in order to reduce the Doppler width. The molecular beam is crossed at right angles in the third chamber with the laser beam 360 mm downstream of the nozzle. The resulting fluorescence is collected perpendicular to the plane defined by laser and molecular beam by an imaging optics set-up consisting of a concave mirror and two plano-convex lenses. The resulting Doppler width in this set-up is 25 MHz (FWHM). The integrated molecular fluorescence is detected by a photo-multiplier tube whose output is discriminated and digitized by a photon counter and transmitted to a PC for data recording and processing. The relative frequency is determined with a quasi-confocal Fabry-Perot interferometer with a free spectral range (FSR) of 149.9434(56) MHz. The FSR has been calibrated using the combination differences of 111 transitions of indole for which the microwave transitions are known [13,14]. The absolute frequency was determined by recording the iodine absorption spectrum and comparing the transitions to the tabulated lines [15].

3. Theoretical methods

The structure of 4-methylstyrene in the electronic ground state has been optimized at the HF/6-31G(d,p), B3LYP/6-31G(d,p), and MP2/6-31G(d,p) levels and at the CIS/6-31G(d,p) level for the electronically excited S_1-state with the GAUSSIAN 98 program package (Revision 11) [16]. The SCF convergence criterion used throughout the calculations was an energy change below 10^{-8} Hartree, while the convergence criterion for the gradient optimization of the molecular geometry was $\partial E/\partial r < 1.5\times10^{-5}$ Hartree/Bohr and $\partial E/\partial\phi < 1.5\times10^{-5}$ Hartree/degrees, respectively. Additionally a CASSCF optimization has been performed with eight electrons in eight orbitals. The active space comprises the six aromatic π, π* orbitals located at the benzene ring, and two π, π* orbitals from the vinyl group.

The barrier for the methyl torsion has been calculated for the ground state at the UMP2/6-31G(d,p) and the B3LYP/6-31G(d,p) level of theory. One dihedral angle of the methyl group is scanned in increments of 5°, while all other geometry parameters are allowed to relax for the respective geometry. The resulting motion is not a simple one-dimensional torsion of the methyl group about the C–C bond but a rather complicated motion, involving more vibrational degrees of freedom. Nevertheless, this motion represents the minimum energy path connecting two minimum structures via a transition state.

4. Results and discussion

The upper trace of Fig. 1 shows the high resolution LIF spectrum of the electronic origin of methylstyrene at 34,277.96 cm^{-1}. The rotationally resolved spectrum contains two torsional subbands due to the internal rotation of the methyl group. The origins of the A↔A and E↔E subbands are marked by arrows in the spectrum. An additional splitting of the electronic origin due to the twofold vinyl torsion cannot be resolved in the spectrum. The experimental spectrum was automatically assigned using a genetic algorithm based fit described in Refs. [9,10]. The cost function used to describe the quality of the fit was defined as $C_{fg}=100(1-F_{fg})$ with the fitness function F_{fg}:

$$F_{fg} = \frac{(\boldsymbol{f},\boldsymbol{g})}{||\boldsymbol{f}||\,||\boldsymbol{g}||}. \tag{1}$$

Here f and g represent the experimental and calculated spectra, respectively, and the inner product $(\boldsymbol{f},\boldsymbol{g})$ is defined with the metric $\boldsymbol{W}$ which has the matrix elements $W_{ij}=w(|j-i|)=w(r)$ as:

$$(\boldsymbol{f},\boldsymbol{g}) = \boldsymbol{f}^{\mathrm{T}}\boldsymbol{W}g, \tag{2}$$

and the norm of $\boldsymbol{f}$ as $||\boldsymbol{f}||=\sqrt{(\boldsymbol{f},\boldsymbol{f})}$ and similar for $\boldsymbol{g}$. For $w(r)$ we used a triangle function [9] with a width of the base of Δw:

$$w(r) = \begin{cases} 1-|r|/\left(\frac{1}{2}\Delta w\right) & \text{for } |r| \le \frac{1}{2}\Delta w \\ 0 & \text{otherwise.} \end{cases} \tag{3}$$

The simulation, using the best fit parameters is shown in the second trace of Fig. 1. We used the GA library PGAPack

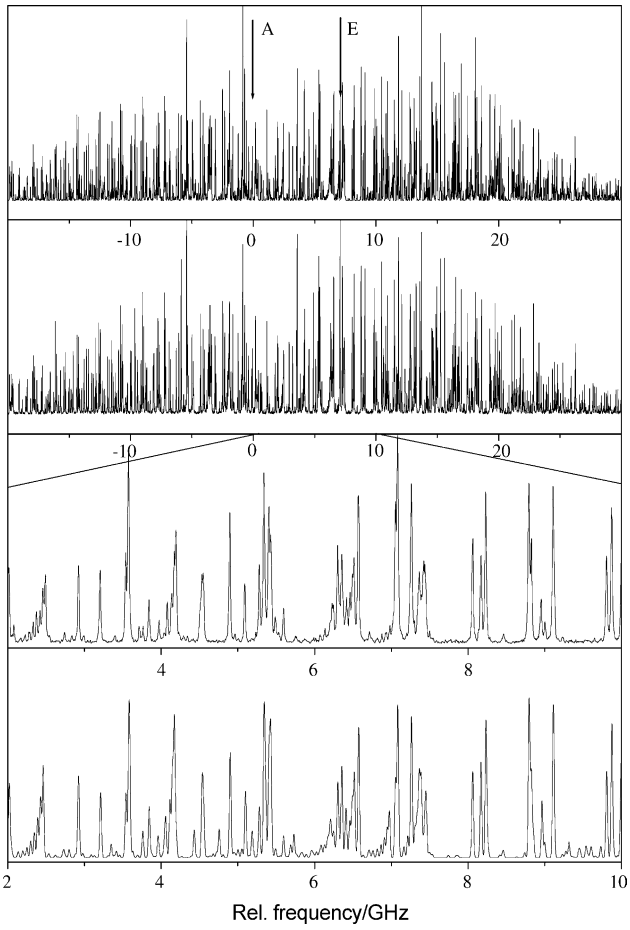

Fig. 1. Rotationally resolved LIF spectrum of the electronic origin of 4-methylstyrene. The frequencies are given relative to the frequency of the electronic origin. The upper trace shows the experimental spectrum, the lower trace the simulation.

version 1.0, which can run on parallel processors [17]. The calculations were performed on eight processors of a SUN UltraSPARC 333 MHz and on a 2.6 GHz PC with two processors under Linux. The genetic algorithm uses concepts copied from natural reproduction and selection processes. For a detailed description of the GA the reader is referred to the original literature on evolutionary or genetic algorithms [18–20]. Since the GA performs an intensity fit of the complete spectrum, much better information on the dipole moment orientation and line width parameters is gathered than from an intensity fit to a few individual lines. Thus, the GA results in improved values for the in plane angle θ that is connected to the planar components of the transition dipole moment (TDM) by:

$$\mu_a = \mu \cos\theta, \quad \mu_b = \mu \sin\theta \tag{4}$$

The angle θ (see Fig. 2 for definition) of the transition dipole moment with the inertial a-axis is determined from the GA fit to be $\pm 16.04°$. The program uses the two temperature model [21]:

$$n(T_1, T_2, w_T) = \mathrm{e}^{-E/kT_1} + w_T \mathrm{e}^{-E/kT_2}. \tag{5}$$

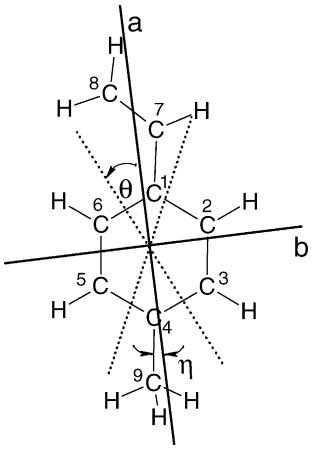

Fig. 2. Atomic numbering, inertial axes of 4-methylstyrene and the definitions of the angles η (angle of the torsional axis with the a-axis) and θ (angle of the transition dipole moment with the a-axis).

Here E is the energy of the lower state, w_T a weight factor, and T_1 and T_2 the two temperatures.

The lineshapes were fit using a Voigt profile [22] with a fixed Gaussian contribution of 25 MHz. The resulting Lorentz width is 5.7 ± 1 MHz. This corresponds to a S_1 state life time of 30 ± 7 ns compared to 20 ns for styrene. All results are summarized in Table 1.

4.1. Barrier to internal rotation of the methyl group

The coupling between the internal rotation of the methyl group and the overall rotation of the molecule is treated in the formalism of the principal axis method (PAM) [23,24]. The Hamiltonian for a molecule with simultaneous internal and overall rotation is:

$$\hat{H} = \hat{H}_R + \hat{H}_T + \hat{H}_{RT} \tag{6}$$

where $\hat{H}_R$ is the pure rigid rotational Hamiltonian:

$$\hat{H}_R = AJ_a^2 + BJ_b^2 + CJ_c^2 \tag{7}$$

Table 1
Molecular parameters of 4-methylstyrene from a combined fit of the rovibronic spectrum and the torsional bands

	S_0	S_1
A (MHz)	4969.63(51)	4763.87(80)
B (MHz)	980.29(4)	997.74(15)
C (MHz)	822.72(4)	816.05(14)
V_3 (cm^{-1})	23.22(11)	−16.99(16)
V_6 (cm^{-1})	−14.31(158)	−6.83(220)
F (cm^{-1})	5.253(18)	5.187(7)
η (deg)	6.55(6)	7.32(20)
ν_0 (cm^{-1})		34,277.96(4)
T_1 (K)	1.54	
T_2 (K)	3.55	
W	0.08	
θ (deg)	16.46	
$\Delta_{Lorentz}$ (MHz)	5.7	

For details see text.

and $\hat{H}_T$ is the pure torsional Hamiltonian

$$\hat{H}_T = Fp^2 + \frac{1}{2}\sum_{n=1}^{2} V_{3n}(1 - \cos 3n\alpha) \tag{8}$$

which depends only on the torsional angle α and can therefore be separated if the coupling is small and $\hat{H}_{RT}$ can be treated by perturbation theory. F is the torsional constant and defined by:

$$F = \frac{h}{8\pi^2 r I_\alpha} \tag{9}$$

with

$$r = 1 - \sum_{g=a,b,c} \frac{\lambda_g^2 I_\alpha}{I_g} \tag{10}$$

where the λ_g are the direction cosines between the inertial axes and the axis of internal rotation. I_α is the moment of inertia of the internal rotor with respect to its symmetry axis and the I_g are the principal moments of inertia of the entire molecule. The second term in Eq. (8) gives the potential energy expanded in a series of $3n$-fold potentials.

The third term $\hat{H}_{RT}$ in Eq. (6) describes the coupling between internal and overall rotation. In the high barrier limit this coupling term is small and can be evaluated by perturbation theory. It yields the torsion–rotation Hamiltonian [23,25]:

$$\hat{H}_{RT} = FW_{v\sigma}^{(1)}(\rho_a J_a + \rho_b J_b + \rho_c J_c) + FW_{v\sigma}^{(2)}(\rho_a J_a + \rho_b J_b + \rho_c J_c)^2 \tag{11}$$

where the first order perturbation coefficients $W_{v\sigma}^{(1)}$ are zero for the nondegenerate A-levels, while $W_{v\sigma}^{(2)}$ is nonzero for both A and E levels. The coefficients ρ_g with g$=a,b,c$ are defined as

$$\rho_g = \lambda_g \frac{I_\alpha}{I_g} \tag{12}$$

Rather than expressing ρ_g in the directional cosines λ_g we can rewrite Eq. (12) in terms of the polar angles (ζ,η). Here η is the angle between the projection vector of the three-fold rotor axis on the ab-plane and the a-axis (see Fig. 2) and ζ the angle between the three-fold rotor axis and the c-axis. We than can write:

$$\rho_a = I_\alpha/I_a \sin\zeta\cos\eta, \quad \rho_b = I_\alpha/I_b \sin\zeta\sin\eta, \quad \rho_c = I_\alpha/I_c \cos\zeta. \tag{13}$$

The n-th order perturbation coefficients $W_{v\sigma}^{(n)}$ in Eq. (11) are defined by [23]:

$$W_{v\sigma}^{(0)} = \frac{E_{v\sigma}}{F} \tag{14}$$

$$W_{v\sigma}^{(1)} = -2\langle v,\sigma|p|v,\sigma\rangle \tag{15}$$

$$W_{v\sigma}^{(2)} = 1 + 4F\sum_{v'} \frac{|\langle v,\sigma|p|v',\sigma\rangle|^2}{E_{v\sigma} - E_{v'\sigma}} \tag{16}$$

where $|v,\sigma\rangle$ are eigenfunctions of Eq. (8) and $E_{v\sigma}$ are the respective eigenvalues with v as the torsional state index. $\sigma = 0, \pm 1$ is chosen in such a way that it represents the symmetry of the torsional wavefunctions and therefore the torsional problem is diagonal in σ. For even v the absolute value of σ increases with increasing energy, while the order is reversed for odd values of v.

The rovibronic spectrum, which is perturbed by the torsion can be fit to the sum of rotational Hamiltonian (Eq. (7)) and torsion–rotation Hamiltonian (Eq. (11)) using the definitions of the first and second-order perturbation coefficients given in Eqs. (15) and (16). Additional information about the barriers and torsional constants is contained in the frequencies of the torsional bands in the ground and electronically excited state. They can be calculated as eigenvalues of Eq. (8). In a recent paper [26], it was shown how the combination of low resolution torsional bands and higher order perturbation coefficients from high resolution spectroscopy can be used in a combined fit to give accurate and uncorrelated barriers and torsional constants for both electronic states. Thus, for methylstyrene the following seven parameters have to be fit for each electronic state: A, B, C, V_3, V_6, F, and η. As the methyl rotor is placed in the plane of the aromatic, the angle ζ was fixed to 90°. Table 1 gives the results of the combined fit. The torsional transitions from Ref. [2], which are used in the fit are summarized in Table 2. The apparent larger deviations for the higher torsional bands might be due to the assumption of a constant absolute uncertainty throughout the spectrum.

4.2. Determination of the structure

The program *pKrFit* [27] was used to determine the structure of 4-methylstyrene in the S_0 and S_1-states from the rotational constants, given in Table 1. Due to the very

Table 2
Torsional transitions of 4-methylstyrene from Ref. [2] and fit, using the parameters from Table 1

4-Methylstyrene	Exp.	Fit	
1e ← 1e	7172.1(2)[a]	7172.062	MHz
2e ← 1e	16(2)	18.27	cm^{-1}
$3a_1 \leftarrow 0a_1$	50(2)	51.14	cm^{-1}
2e → 1e	20.3(10)	18.700	cm^{-1}
$0a_1 \rightarrow 3a_2$	45.1(10)	46.31	cm^{-1}
$0a_1 \rightarrow 3a_1$	52.8(10)	54.66	cm^{-1}
4e → 1e	83.0(10)	81.87	cm^{-1}
5e → 1e	135.7(10)	129.94	cm^{-1}
$0a_1 \rightarrow 6a_1$	192.0(10)	196.78	cm^{-1}

The electronic transitions are labelled by the m quantum number and the symmetry of the subtorsional level σ: $m\sigma(S_1) \leftarrow m\sigma(S_0)$ for absorption bands and $m\sigma(S_1) \rightarrow m\sigma(S_0)$ for emission bands.

[a] Experimentally determined AE-splitting (this work).

limited number of inertial parameters, we performed a fit limited to the r_0-structure, which neglects the vibrational contributions from the different isotopomers and which is based on the assumption:

$$I_0^g = I_{\text{rigid}}^g(r_0) \tag{17}$$

I_0^g are the (experimentally determined) zero-point averaged moments of inertia with respect to the inertial axes g. The functions $I_{\text{rigid}}^g(r_0)$ are calculated from the structural parameters r_0 using rigid-molecule formulas. Thus no vibrational corrections are introduced in the determination of the structure.

Fig. 2 gives the atomic numbering used in the fit of the structure. In order to reduce the number of fit parameters we set the C_1–C_2 bond equal to C_6–C_1, C_2–C_3 equal to C_5–C_6, and C_3–C_4 equal to C_4–C_5. All aromatic CH bonds are set to the same value (107.7 pm for the ground state and 107.4 pm for the excited state). The vinyl CH bonds are set to 107.5 pm, the methyl CH bonds to 108.5 pm for both electronic states. The dihedral angles are chosen to give a planar structure in both electronic states. The structural parameters that were fit, are the C_1–C_2, the C_2–C_3 and the C_3–C_4 bond of the aromatic ring. In the electronic ground state the three bonds are nearly equal (139.7(2), 139.6(5), and 139.7(4), respectively). In the electronically excited state the ring expands, while the C_2–C_3 bond length decreases (143.8(2), 138.5(3), and 143.6(2), respectively). Of course, this geometry change is a tentative one, regarding the large number of parameters which had to be fixed and set to average values.

4.3. Comparison to the results of ab initio calculations

4.3.1. Structure

Table 3 compares the results of the experimentally determined rotational constants to the results of various ab initio calculations The experimental ground state rotational constants are numerically in good agreement with the results of the MP2/6-31G(d,p) and the B3LYP/6-31G(d,p) optimized structures. While the B3LYP calculation reproduces the experimentally determined planarity of the vinyl group (calculated inertial defect 3.128 μÅ^2), the MP2 calculation yields an out-of-plane angle of 26.2° (calculated inertial defect −8.1 μÅ^2). The large barrier for the torsional motion of the vinyl group determined by Hollas et al. [2] excludes the possibility of a torsionally averaged planar structure at the temperature of our molecular beam. This situation is similar to styrene, in which the planar MP2 optimized structure has been found to be a first-order saddle point, while the B3LYP structure is a real minimum on the potential energy surface. In case of methylstyrene, we found the all-planar structure (with the methyl group eclipsed) to be a second-order saddle point. The two imaginary frequencies describe the transit of the out-of-plane vinyl and methyl groups through the planar transition state. The fully optimized MP2 structure exhibits an out-of-plane angle of 26.2° for the vinyl group and of 29.3° for the methyl group (staggered conformation). The change of rotational constants upon electronic excitation can be approximated by the difference of optimized HF and CIS calculations using the same basis set. More accurate values for the changes of the rotational constants are obtained from the CASSCF(8/8) calculations. The ab initio structures for both electronic states are compared to the results of the geometry fit, which is described in Section 4.2. Due to the limited number of structure parameters which could be fit, the mean values of the bond lengths on both sides of the ring have been taken as results of the ab initio calculations in Table 4. Theory and experiment agree well in a benzoid structure for the ground state with all ring bond lengths equal and in the quinoidal distortion of the aromatic ring upon excitation, that is typical for *para*-disubstituted aromatics. The largest expansion is found for the C_1–C_2 bond, which is in vicinity to the vinyl group. The 'middle' bonds of the aromatic ring nearly remain constant of even contract slightly, while the C_2–C_3 bond length expands.

Table 3
Experimental and ab initio inertial constants of 4-methylstyrene

	Exp.	MP2	B3LYP	HF	CIS	CIS-HF	CAS (8/8)
A''	4969.63	4941	4952	5017	–	–	4965[a]
B''	980.29	980	975	984	–	–	974[a]
C''	822.72	822	818	829	–	–	818[a]
A'	4763.87	–	–	–	4736	–	4761[b]
B'	997.74	–	–	–	1005	–	959[b]
C'	816.05	–	–	–	833	–	802[b]
ΔA	−205.76	–	–	–	–	−281	−204
ΔB	−0.55	–	–	–	–	+21	−15
ΔC	−6.67	–	–	–	–	+4	−16

All calculations have been performed using the 6-31G(d,p) basis set. All values are given in MHz.
[a] Geometry optimized to the S_0-state.
[b] Geometry optimized to the S_1-state.

4.3.2. Transition dipole moment

The orientation of the TDM with respect to the *a*-axis has been determined experimentally to be $\pm 16 \pm 12°$. Together with the TDM orientation in styrene ($\pm 9 \pm 3°$), this value can be used to distinguish between the two possible orientations. If we assume, that the influence of the methyl group on the orientation of the electronic transition dipole

Table 4
Structural parameters of *p*-methylstyrene

		r_0	CAS(8/8)	HF	CIS
S_0	C_1C_2 (pm)	139.7	139.9	139.6	–
	C_2C_3 (pm)	139.6	139.7	138.3	–
	C_3C_4 (pm)	139.7	139.5	139.0	–
S_1	C_1C_2 (pm)	143.8	145.0	–	145.0
	C_2C_3 (pm)	138.5	142.9	–	136.5
	C_3C_4 (pm)	143.6	142.7	–	142.0

For atomic numbering see Fig. 2.

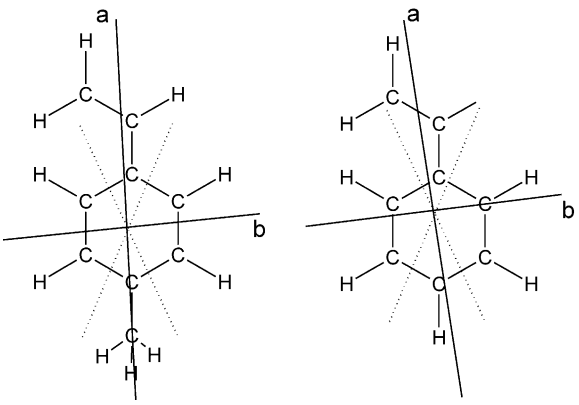

Fig. 3. Orientation of the TDM in 4-MS and styrene (from Ref. [8]). Both orientations of the TDM are shown in the graphs. For styrene, the TDM has been drawn in the same orientation as in 4-MS, and the inertial axis system has been rotated.

is small, we can focus our attention on the rotation of the inertial axes in 4-MS compared to styrene due to the presence of the methyl group. Fig. 3 shows the orientation of the TDM in 4-MS and in styrene. As we postulate only a small electronic perturbation due to the methyl group, the orientations of the TDM are the same in both cases. However, due to the different mass distributions the inertial axes systems are different. As can be inferred from Fig. 3, the angle between the *a*-axis and the TDM should decrease when going from 4-MS to styrene if the TDM is oriented in direction of the vinyl group and should increase otherwise. As the respective angle in styrene is smaller than in 4-MS the TDM should be oriented in direction of the vinyl group (a positive value of the angle).

The CIS calculations yield an TDM angle of $+25°$, where the positive direction is defined as counterclockwise from the *a*-axis towards the TDM. Based on the CASSCF optimized S_0 structure the CAS wavefunctions have been set-up using MOLCAS [28] and the transition dipole moment has been calculated in the geometry of the S_0 state to be $-35°$. Thus, the CIS calculations predict the transition dipole moment to be oriented in direction of the vinyl group, as inferred from the experiment, while the CASSCF calculations predict the dipole moment to point away from the vinyl group.

4.3.3. Barrier to methyl torsion

The barrier for the methyl rotation has been calculated both at the B3LYP/6-31G(d,p) and at the MP2/6-31G(d,p) level of theory. One dihedral angle, defining the orientation of the methyl group with respect to the aromatic frame has been incremented, while all other geometry parameters were optimized in each step. Fig. 4 shows the calculated minimum energy path along the dihedral angle of the methyl group for both methods. The planar B3LYP structure has its minimum at a dihedral of 0° (anti to the orientation of the vinyl group), the nonplanar MP2 structure has its minimum at 26°. The experimentally determined ground state potential given by

$$V = \frac{1}{2}[V_3(1 - \cos 3\alpha) + V_6(1 - \cos 6\alpha)] \quad (18)$$

with $V_3 = 23.22\ \mathrm{cm}^{-1}$ and $V_6 = -14.31\ \mathrm{cm}^{-1}$ is shown for comparison as dotted line in both potentials. The ab initio calculated potentials are drawn by full lines.

The B3LYP calculation yields a predominant V_3 contribution to the barrier while MP2 results in a mixed V_3/V_6 potential with dominant V_6-term. A fit of the ab initio potentials to Eq. (18) gives $V_3 = 19\ \mathrm{cm}^{-1}$ and $V_6 = -3\ \mathrm{m}^{-1}$ for the B3LYP calculations and $V_3 = 6.5\ \mathrm{cm}^{-1}$ and $V_6 = -21\ \mathrm{cm}^{-1}$ for the MP2 barrier.

The experimentally determined potential is dominated by the V_3-term, but with a significantly larger V_6-term than predicted by the B3LYP calculations. Purely steric considerations would prefer a V_6 dominated potential energy, as the vinyl and the methyl group in *para* position do not 'see each other'. A stronger weight of the threefold contribution on the other hand points to electronic ('through ring') explanations for the hindering potential. This 'through ring' interaction should couple then the methyl group torsion to

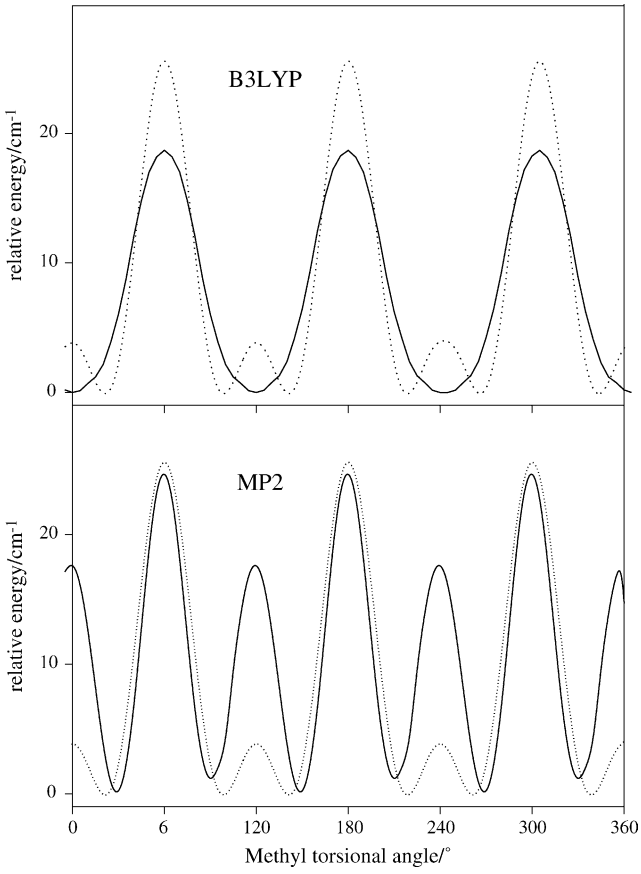

Fig. 4. Ab initio calculated torsional barrier for the methyl rotation of *p*-methylstyrene. All structural parameters are allowed to relax, despite the torsional angle of the methyl group. The full lines give the B3LYP/6-31G(d,p) energy (upper graph) and the MP2/6-31G(d,p) energy (lower graph). The dotted lines show the torsional potential using the parameters from Table 2 for comparison.

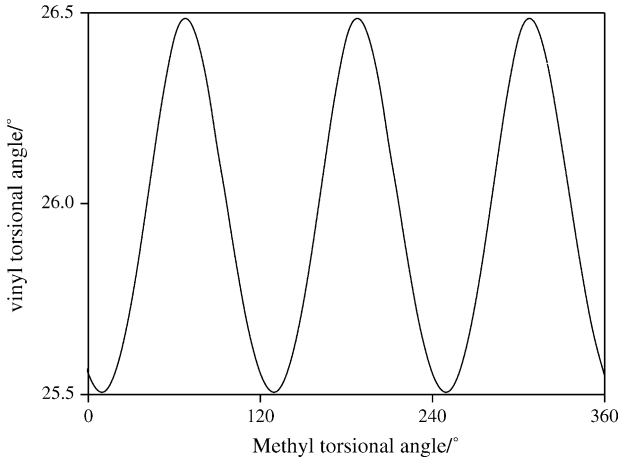

Fig. 5. Dependance of the out-of-plane dihedral angle of the vinyl group from the torsional dihedral angle of the methyl group.

some geometry change of the vinyl group. As all geometry parameters are allowed to relax, their dependence on the torsional angle of the vinyl group can be investigated. Fig. 5 shows how the dihedral (torsional) angle of the vinyl group is coupled to the torsional angle of the methyl group. A variation of the vinyl dihedral angle with the methyl torsional angle is found at MP2 level, although the amplitude is small (about 1°).

5. Conclusions

The structure of 4-methylstyrene is found to be distorted quinoidally upon electronic excitation. The experimentally determined structural changes are very similar to changes obtained from CASSCF calculations for both electronic states and close agreement between experiment and theory is found. The quinoidal distortion is more pronounced than in other *para*-disubstituted aromatic compounds like *p*-fluorophenol [29], *p*-cyanophenol [30], and *p*-methylphenol. This is a consequence of the enhanced tautomerism due to the vinyl group, that stabilizes a quinoidal form.

The barrier to methyl torsion was determined from combined fits of low resolution torsional bands, the experimentally determined AE-splitting and the torsion–rotation perturbation coefficients in both electronic states. The resulting potential is dominated by a threefold barrier with a smaller sixfold contributions. On all accounts, the agreement of the experimentally determined barriers with the ab initio MP2 and B3LYP values is not completely satisfying. While the MP2 calculations overestimate the sixfold part of the potential, it is underestimated by the density functional calculations. The MP2 calculations predict a coupling of the methyl torsion via a through ring interaction to the twofold torsion of the vinyl group in *para* position.

Acknowledgements

The financial support of the Deutsche Forschungsgemeinschaft (SCHM 1043/9-4) is gratefully acknowledged. M. S. likes to thank the Nordrheinwestfälische Akademie der Wissenschaften for a grant which made this work possible. We thank Robert Brause for help with the calculations of the transition dipole moments.

References

[1] J.M. Hollas, P.F. Taday, J. Chem. Soc. Faraday Trans. 86 (1990) 217–218.
[2] J.M. Hollas, P.F. Taday, R.D. Gordon, J. Mol. Spectrosc. 153 (1992) 587–598.
[3] C.H. Choi, M. Kertesz, J. Phys. Chem. A 101 (1997) 3823–3831.
[4] J.M. Granadino-Roldán, M. Fernádez-Gómez, A. Navarro, Chem. Phys. 372 (2003) 255.
[5] V.H. Grassian, E.R. Bernstein, H.V. Secor, J.I. Seeman, J. Phys. Chem. 93 (1989) 3470–3474.
[6] J.C. Cochran, K. Hagen, G. Paulen, Q. Shen, S. Tom, M. Traetteberg, C. Wells, J. Mol. Struct. 413 (1997) 313–326.
[7] W. Caminati, B. Vogelsanger, A. Bauder, J. Mol. Spectrosc. 128 (1988) 384–398.
[8] J.W. Ribblett, D.R. Borst, D.W. Pratt, J. Chem. Phys. 111 (1999) 8454–8461.
[9] J.A. Hageman, R. Wehrens, R. de Gelder, W.L. Meerts, L.M.C. Buydens, J. Chem. Phys. 113 (2000) 7955–7962.
[10] W.L. Meerts, M. Schmitt, G. Groenenboom, Can. J. Chem. 82 (2004) 804–819.
[11] M. Schmitt, C. Ratzer, W.L. Meerts, J. Chem. Phys. 120 (2004) 2752–2758.
[12] M. Schmitt, J. Küpper, D. Spangenberg, A. Westphal, Chem. Phys. 254 (2000) 349–361.
[13] R.D. Suenram, F.J. Lovas, G.T. Fraser, J. Mol. Spectrosc. 127 (1988) 472–480.
[14] W. Caminati, S. di Bernardo, J. Mol. Struct. 240 (1990) 253–262.
[15] S. Gerstenkorn, P. Luc, Atlas du Spectre D'absorption de la Molécule d'iode, CNRS, Paris 1982.
[16] M.J. Frisch, G.W. Trucks, H.B. Schlegel, G.E. Scuseria, M.A. Robb, J.R. Cheeseman, V.G. Zakrzewski, J.A. Montgomery Jr., R.E. Stratmann, J.C. Burant, S. Dapprich, J.M. Millam, A.D. Daniels, K.N. Kudin, M.C. Strain, O. Farkas, J. Tomasi, V. Barone, M. Cossi, R. Cammi, B. Mennucci, C. Pomelli, C. Adamo, S. Clifford, J. Ochterski, G.A. Petersson, P.Y. Ayala, Q. Cui, K. Morokuma, P. Salvador, J.J. Dannenberg, D.K. Malick, A.D. Rabuck, K. Raghavachari, J.B. Foresman, J. Cioslowski, J.V. Ortiz, A.G. Baboul, B.B. Stefanov, G. Liu, A. Liashenko, P. Piskorz, I. Komaromi, R. Gomperts, R.L. Martin, D.J. Fox, T. Keith, M.A. Al-Laham, C.Y. Peng, A. Nanayakkara, M. Challacombe, P.M.W. Gill, B. Johnson, W. Chen, M.W. Wong, J. Andres, C. Gonzalez, M. Head-Gordon, E.S. Replogle, J.A. Pople, GAUSSIAN 98, revision a.11, Gaussian, Inc., Pittsburgh, PA, 2001.
[17] D. Levine, PGAPack V1.0, PgaPack can be obtained via anonymous ftp from: ftp://ftp.mcs.anl.gov/pub/pgapack/pgapack.tar.z.
[18] J.H. Holland, Adaption in Natural and Artificial Systems, The University of Michigan Press, Ann-Arbor, MI, 1975.
[19] D.E. Goldberg, Genetic Algorithms in Search, Optimisation and Machine Learning, Addison-Wesley, Reading, MA, 1989.

[20] I. Rechenberg, Evolutionsstrategie—Optimierung Technischer Systeme Nach Prinzipien der Biologischen Evolution, Frommann-Holzboog, Stuttgart, 1973.
[21] Y.R. Wu, D.H. Levy, J. Chem. Phys. 91 (1989) 5278–5284.
[22] W. Voigt, Sitzungsber. Math. Naturwiss. KI. bayer. Akad. Wiss. 1912;603.
[23] W. Gordy, R.L. Cook, Microwave Molecular Spectra, third ed., Wiley, New York, 1984.
[24] C.C. Lin, J.D. Swalen, Rev. Mod. Phys. 31 (1959) 841–891.
[25] D.R. Herschbach, J. Chem. Phys. 31 (1959) 91–108.
[26] C. Jacoby, M. Schmitt, Chem. Phys. Chem. 5 (2004) 1686–1694.
[27] C. Ratzer, J. Küpper, D. Spangenberg, M. Schmitt, Chem. Phys. 283 (2002) 153–169.
[28] K. Andersson, M. Barysz, A. Bernhardsson, M.R.A. Blomberg, D.L. Cooper, M.P. Fülscher, C. de Graaf, B.A. Hess, G. Karlström, R. Lindh, P.-A. Malmqvist, T. Nakajima, P. Neogrády, J. Olsen, B.O. Roos, B. Schimmelpfennig, M. Schütz, L. Seijo, L. Serrano-Andrés, P.E.M. Siegbahn, J. Stalring, T. Thorsteinsson, V. Veryazov, P.-O. Widmark, Molcas Version 5.4, Lund University, Sweden, 2002.
[29] C. Ratzer, M. Nispel, M. Schmitt, Phys. Chem. Chem. Phys. 5 (2002) 812.
[30] J. Küpper, M. Schmitt, K. Kleinermanns, Phys. Chem. Chem. Phys. 4 (2002) 4634.